Relativistic space-charge-limited current for massive Dirac fermions

Y. S. Ang,[*] M. Zubair,[†] and L. K. Ang[‡]

SUTD-MIT International Design Center, Singapore University of Technology and Design, Singapore 487372

(Received 12 August 2016; revised manuscript received 10 March 2017; published 7 April 2017)

A theory of relativistic space-charge-limited current (SCLC) is formulated to determine the SCLC scaling, $J \propto V^{\alpha}/L^{\beta}$, for a finite band-gap Dirac material of length L biased under a voltage V. In one-dimensional (1D) bulk geometry, our model allows (α,β) to vary from (2,3) for the nonrelativistic model in traditional solids to (3/2,2) for the ultrarelativistic model of massless Dirac fermions. For 2D thin-film geometry we obtain $\alpha = \beta$, which varies between 2 and 3/2, respectively, at the nonrelativistic and ultrarelativistic limits. We further provide rigorous proof based on a Green's-function approach that for a uniform SCLC model described by carrier-density-dependent mobility, the scaling relations of the 1D bulk model can be directly mapped into the case of 2D thin film for any contact geometries. Our simplified approach provides a convenient tool to obtain the 2D thin-film SCLC scaling relations without the need of explicitly solving the complicated 2D problems. Finally, this work clarifies the inconsistency in using the traditional SCLC models to explain the experimental measurement of a 2D Dirac semiconductor. We conclude that the voltage scaling $3/2 < \alpha < 2$ is a distinct signature of massive Dirac fermions in a Dirac semiconductor and is in agreement with experimental SCLC measurements in MoS_2.

DOI: 10.1103/PhysRevB.95.165409

I. INTRODUCTION

Space-charge-limited current (SCLC) gives the maximum current that can be transported across a solid of length L with a biased voltage V, limited by the electrostatic repulsion generated by the *in-transit* unscreened charge carriers that are in excess of the thermodynamically allowed population [1]. In a trap-free bulk crystal, SCLC exhibits a signature current-voltage (J-V) characteristic of $J_{\mathrm{MG}} \propto V^2/L^3$, known as the Mott-Gurney (MG) law [2], which is the solid-state counterpart of the SCLC in vacuum as given by the Child-Langmuir (CL) law: $J_{\mathrm{CL}} \propto V^{3/2}/L^2$ in the classical regime [3,4] and $J_{\mathrm{CL}} \propto V^{1/2}/L^4$ in the quantum regime [5,6]. Including defect states or traps in solids, SCLC becomes *trap-limited* as described by the Mark-Helfrich (MH) law [7]: $J_{\mathrm{MH}} \propto V^{l+1}/L^{2l+1}$, where $l = T_c/T$ (T is the temperature and T_c is a parameter characterizing the exponential spread in energy of the traps). Due to the geometrical effect [8], the one-dimensional (1D) SCLC value is enhanced as a result of a finite emission area [9] and weakened Coulomb screening in a high aspect-ratio nanowire [10]. Furthermore, SCLC is an important tool to probe the trap characteristics in solids, and also for photocurrent measurement since the extraction efficiency of photogenerated carriers is fundamentally limited by SCLC [11].

For organic semiconductors, field-dependent [12–15] and density-dependent mobility SCLC models [16,17] are commonly employed to characterize the SCLC carried by the holes. Similarly, SCLC of electrons was found to be universally described by a trap model with Gaussian energy distribution in a large class of organic semiconductors [18,19]. Recently, it was demonstrated that the magnitude of electron SCLC can be significantly enhanced via the dilution of traps in conjugated polymer blends of only 10% active semiconductors [20], which opens up an exciting possibility of a high-efficiency and low-cost organic light-emitting diode. SCLC in the trap-limited regime was reformulated [21] with the inclusion of the interplay between dopants and traps, the Poole-Frenkel effect [22], and quantum-mechanical tunneling, which solved the long-standing problem [23,24] of the enormously sharp current rise in the trap-limited regime, and it demonstrated that an exponentially distributed trap is not necessarily required to explain the power-law sharp rises of SCLC in the trap-limited regime. Remarkably, the model successfully reproduced the anomalous noise-spectrum peak observed in [25].

In spite of SCLC being a classic model first derived in the 1940s, it remains an active topic for organic materials and nanowires, as mentioned above. With the advances in fabricating novel 2D Dirac materials [26–28], it is of interest to revisit the SCLC model for these 2D Dirac materials. To the best of our knowledge, there is no theory or model to deal with the SCLC transport in Dirac materials. Recent experiments reported a typical J-V characteristic in the form of MH law for highly disordered materials such as reduced graphene oxide [29,30]. On the other hand, SCLC in a crystalline monolayer MoS_2 [31] and hBN [32] was found to exhibit an unusual power-law dependence of $J \propto V^{\alpha}$ with $1.7 \lesssim \alpha \lesssim 2.5$, which was claimed to originate from the different levels of traps in different samples by using the traditional MH law. This explanation is doubtful as the traditional MH law is only valid for $\alpha > 2$ for $T_c > T$, which implies that the voltage scaling from the MH law must be $\alpha \geqslant 2$ theoretically and it cannot be used to fit with the measured scaling of $1.7 \lesssim \alpha \lesssim 2.5$. For $T_c < T$, the traps are narrowly distributed in energy space and the SCLC essentially reduces to single-level shallow trapping with $\alpha = 2$ [23]. Thus, the observation of $\alpha < 2$ cannot be explained by the MH law or other SCLC models such as a shallow trap [23], Gaussian disorder [33], field-dependent mobility [12], and density-dependent [16] mobility.

For a Dirac material with a finite band gap, the electrons mimic relativistic *massive Dirac fermions* [34,35], whereas the classical SCLC models are based on the conduction model

[*]Corresponding author: yeesin_ang@sutd.edu.sg

[†]On leave of absence from Faculty of Electrical Engineering, GIK Institute of Engineering Sciences and Technology, Topi 23640, Pakistan.

[‡]Corresponding author: ricky_ang@sutd.edu.sg

of *nonrelativistic* quasifree electrons [1]. In this work, we proposed a model of *relativistic* SCLC of massive Dirac fermions, which can explain the peculiar $\alpha < 2$ scaling observed in recent experiments using Dirac materials, and thus it circumvents the unjustified assumption of $T_c < T$ used in the MH law in order to fit the experimental data. According to our model, the J_1-V characteristics of SCLC in a 1D bulk geometry will vary between the nonrelativistic limit of $J_1 \propto V^2/L^3$ and the ultrarelativistic limit of $J_1 \propto V^{3/2}/L^2$ (this is different from the CL law; see below for an explanation). We present a master equation that is in good agreement with the experimental data and can be used to characterize the transition between Ohmic conduction and the SCLC regime. By extending the bulk 1D model to a 2D thin-film model, the scaling relation becomes $J \propto V^{\alpha}/L^{\beta}$, with $\alpha = \beta$ varying between 3/2 and 2, respectively, at the ultrarelativistic and nonrelativistic limits. In doing so, we prove rigorously, using a Green's-function approach [8], that the 1D bulk SCLC current-voltage scaling relation can be directly mapped to 2D thin-film SCLC. It is shown that for a general transport equation of $J = en\mu(n)E$, where $\mu(n)$ is a mobility that depends on carrier density, n, and E is the electric field, the 1D bulk SCLC and 2D thin-film SCLC are linked by a universal SCLC scaling relation (see Sec. III). Our analysis provides a convenient tool to deduce the 2D thin-film SCLC scaling relation via a simple 1D SCLC model without the need of explicitly solving the complicated 2D SCLC model.

II. THEORY OF RELATIVISTIC SPACE-CHARGE-LIMITED CURRENT

In this section, a relativistic SCLC model is developed using the semiclassical Boltzmann transport equation (BTE). For simplicity, we first consider the SCLC by assuming a simple 1D Poisson equation, which allows semianalytical scaling relations to be determined. In Sec. III, we shall show that the simple 1D SCLC scaling relation derived in this section can be directly mapped to the case of 2D SCLC with thin-film geometry.

A. Boltzmann transport equation for a conventional semiconductor

The starting point of the trap-free SCLC theory, i.e., the Mott-Gurney law, is the semiclassical BTE, which provides a basic equation of current density governing the transport of charge carriers. The diffusion component is usually not considered except in some cases of polymers due to their highly disordered nature. For a quasistatic system, the BTE in the linearized transport regime under relaxation-time approximation is

$$-\frac{e\mathbf{E}}{\hbar}\cdot\frac{\partial f}{\partial \mathbf{k}} + \mathbf{v}\cdot\frac{\partial f}{\partial \mathbf{r}} = -\frac{f - f_0}{\tau}, \tag{1}$$

where $\mathbf{E}$ is the electric field, $\mathbf{k}$ is the crystal momentum, $\mathbf{r}$ is the position vector, $\mathbf{v}$ is the carrier velocity, f is the out-of-equilibrium distribution function, f_0 is the equilibrium Fermi-Dirac distribution function, and τ is a typical collision time scale. If the system is spatially homogeneous, the diffusion component of the transport current, i.e., $\partial f/\partial \mathbf{r}$, can be omitted. By assuming a 3D isotropic parabolic energy dispersion, one arrives at the well-known drift-current density, $J = e/(3\pi)^3 \int v_k f d^3\mathbf{k}$, for semiconductors:

$$J_{3D} = \frac{\tau e^2}{m} n(x) E(x). \tag{2}$$

By connecting the drift equation with the 1D Poisson equation via charge density $n(x)$, the Mott-Gurney current-voltage scaling of $J \propto V^2$ can be recovered.

For 2D gapped Dirac materials, Eq. (2) is no longer valid due to two reasons: (i) the dimensionality is reduced to two dimensions, and (ii) the energy dispersion follows a relativistic dispersion similar to that of the massive Dirac fermions. In the following, we shall formulate the drift-equation for Dirac semiconductor based on the BTE approach and demonstrate that the SCLC mediated by relativistic quasiparticles follows a completely different current-voltage scaling relation.

B. Boltzmann transport equation for a 2D Dirac semiconductor

For massive Dirac fermions, the energy dispersion is $\varepsilon_k = \sqrt{\hbar^2 v_F^2 k^2 + \Delta^2}$, where v_F is the Fermi velocity, k is the crystal momentum, and 2Δ is the band gap. The group velocity is $v_k = \hbar^{-1} d\varepsilon_k/dk = \hbar v_F^2 k/\varepsilon_k$. The density of states, $D(\varepsilon) = \sum_{\mathbf{k}} \delta(\varepsilon - \varepsilon_k)$, is rewritten as $D(\varepsilon) = (g_{sv}\varepsilon/2\pi\hbar^2 v_F^2)\Theta(\varepsilon - \Delta)$, where g_{sv} denotes the spin-valley degeneracy and $\Theta(x)$ is a Heaviside function. The electron density at low temperature can then be obtained from the 2D density of states, $n = \int D(\varepsilon_k) d\varepsilon_k$, which gives $n = (g_{sv}/4\pi\hbar^2 v_F^2)(\mu^2 - \Delta^2)$, and μ is the Fermi level. The general expression of the 2D linear current density is $J = (\tau e^2 E/2\pi)\int v_k^2 k\, dk(-\partial f_0/\partial \varepsilon_k)$, where f_0 is the Fermi-Dirac distribution function, τ is the scattering time, and E is the externally applied electric field. In the low-temperature limit, the current density can be analytically solved to give $J = (g_{sv}\tau e^2 E/2\pi\hbar^2\mu)(\mu^2 - \Delta^2)$. Eliminating μ via n, we obtain

$$J = \sqrt{\frac{e g_{sv}}{\pi}}\frac{\tau e v_F}{\hbar}\frac{en(x)}{\sqrt{en(x) + \rho_c}}E(x), \tag{3}$$

where $\rho_c \equiv e g_{sv}\Delta^2/4\pi\hbar^2 v_F^2$ is a band-gap-dependent *characteristic charge density*, and n and E are reexpressed as functions of the transport direction, x. The term $[en(x) + \rho_c]^{-1/2}$ in Eq. (3) represents a major difference between the relativistic massive Dirac fermions and that of the nonrelativistic quasifree electrons. As $\rho_c \propto \Delta^2$, it can be seen from the ε_k-k relation that the electrons are nonrelativistic at very large ρ_c or $\Delta \gg \hbar v_F k$. For vanishingly small ρ_c or $\Delta \ll \hbar v_F k$, the electrons approach an ultrarelativistic limit and become *massless* Dirac fermions.

By expressing Eq. (1) in the Drude form of $J = en\mu_D(n)E$, a density-dependent *Dirac mobility* is defined as $\mu_D \equiv \gamma[en(x) + \rho_c]^{-1/2}$, where $\gamma \equiv \tau v_F e^{3/2} g_{s,v}^{1/2}/\pi^{1/2}\hbar$. Consequently, the relativistic SCLC of massive Dirac fermions belongs to the class of *density-dependent mobility* SCLC. However, $\mu_D \equiv \gamma[en(x) + \rho_c]^{-1/2}$ is unique to the massive Dirac fermions.

C. Relativistic SCLC in bulk geometry

We assume that the SCLC is carried solely by electrons injected through an Ohmic contact. For simplicity, we

employ the 1D Poisson equation $dE(x)/dx = en(x)/\epsilon d$, where $E(x) = dV(x)/dx$, $V(x)$ is the electrostatic potential, and ϵ is the effective dielectric constant. Here, we first assume that the 3D carrier density, $n_{3D}(x)$, is related to $n(x)$ via $n_{3D}(x) = n(x)/d$, with d as an effective thickness (see the modification presented later). By coupling Eq. (3) with the Poisson equation via $n(x)$, we obtain the governing equation of the relativistic SCLC for a Dirac solid:

$$E(x)\frac{dE(x)}{dx} = \frac{J}{\gamma\epsilon d}\sqrt{\epsilon d\frac{dE(x)}{dx} + \rho_c}. \tag{4}$$

We first investigate the solutions of the 1D relativistic SCLC, i.e., Eq. (4), in two asymptotic limits: (i) the nonrelativistic SCLC regime [$\rho_c \gg en(x)$], and (ii) the ultrarelativistic SCLC regime [$\rho_c \ll en(x)$], which allows Eq. (3) to be approximated, respectively, as

$$J_{nr} = \frac{9}{8}\epsilon d\frac{2\tau e v_F^2}{\Delta}\frac{V^2}{L^3}, \quad \rho_c \gg en(x), \tag{5a}$$

$$J_r = \frac{8}{3}\sqrt{\frac{eg_{sv}\delta\epsilon}{3\pi}}\frac{\tau e v_F}{\hbar}\frac{V^{3/2}}{L^2}, \quad \rho_c \ll en(x). \tag{5b}$$

The MG scaling is readily recovered from the nonrelativistic charge dynamics at large ρ_c. As the electrons reside just slightly above the band gap where the inequality $\hbar v_F k \ll \Delta$ holds true, we have $\varepsilon_k \approx m^* v_F^2 + \hbar^2 k^2/2m^*$, where $m^* \equiv \Delta/v_F^2$. It can be shown [36] that the corresponding current density is in the nonrelativistic Drude form, which recovers the MG scaling of $J \propto V^2/L^3$.

In the opposite limit of $\rho_c \to 0, \hbar v_F k \gg \Delta$ implies ultrarelativistic dynamics with a scaling of $J \propto V^{3/2}/L^2$, as shown in Eq. 3(b). Coincidentally, this has the same scaling to the CL law [3], although the underlying physics is fundamentally different. For Dirac materials studied there, the ultrarelativistic SCLC is obtained from

$$J_r \propto \sqrt{\frac{d^2V(x)}{dx^2}}\frac{dV(x)}{dx}, \tag{6}$$

while SCLC in vacuum (or CL law) is obtained from

$$J_{vac} \propto \sqrt{V(x)}\frac{d^2V(x)}{dx^2}. \tag{7}$$

A simple dimensional analysis [37] immediately shows that J_r and J_{vac} are both proportional to $V^{3/2}$ despite their very different origins. Nonetheless, Eq. (6) originates from the $J_r \propto \sqrt{n(x)}$ dependence due to the *ultrarelativistic* electron dynamics in Dirac solids, while Eq. (7) originates from the $J_{vac} \propto \sqrt{V(x)}$ dependence due to the energy balance of a *nonrelativistic* free electron accelerating in vacuum. This demonstrates the fundamentally different mechanism behind the $J \propto V^{3/2}$ scaling in the two cases.

The two limits—$\alpha = 3/2$ and 2—are, respectively, the extreme limits of the ultrarelativistic and nonrelativistic SCLC; an intermediate regime of $3/2 < \alpha < 2$ is expected in the case of massive Dirac fermions. This is in good agreement with the experimental observations of $1.7 < \alpha < 2.5$ in monolayer MoS_2 [31] and $1.75 < \alpha < 2.5$ in monolayer hBN [32], where the charge carriers are essentially massive Dirac fermions. The model proposed here suggests that the $\alpha < 2$ scaling is *intrinsic* to the relativistic carriers without the unjustified or

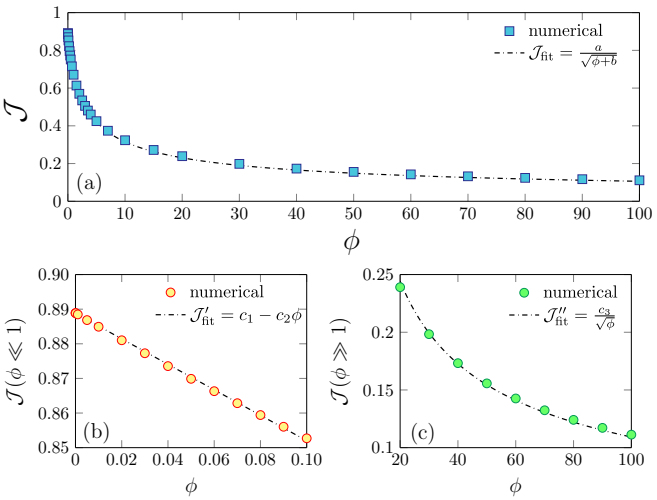

FIG. 1. $\mathcal{J}$ as a function of ϕ. (a) Numerical results of $\mathcal{J}$ over the full range of ϕ. The dashed line shows the empirical fitting equation; numerical results with (b) $\phi \ll 1$; and at (c) $\phi \gg 1$. The fitting constants (a, b, c_1, c_2, and c_3) are (1.067, 1.45, 0.889, 0.368, and 1.092).

invalid assumption of introducing traps with $T_c < T$, which is also inconsistent with the original formulation of the MH law and other trap-limited SCLC models, as discussed above.

For convenience, we transform Eq. (4) into a dimensionless form of

$$\frac{d\mathcal{V}(\chi)}{d\chi}\frac{d^2\mathcal{V}(\chi)}{d\chi^2} = \mathcal{J}\sqrt{\frac{d^2\mathcal{V}(\chi)}{d\chi^2} + \phi}, \tag{8}$$

where $\mathcal{V}(x) \equiv V(x)/V$ and $\chi \equiv x/L$. The normalized current $\mathcal{J}$ and the dimensionless parameter ϕ are

$$\mathcal{J} \equiv \frac{\hbar}{\tau e^{3/2} v_F\sqrt{\epsilon d}}\frac{JL^2}{V^{3/2}}, \tag{9a}$$

$$\phi \equiv \frac{\rho_c}{\epsilon d}\frac{L^2}{V}. \tag{9b}$$

For a given value of ϕ and boundary conditions, $\mathcal{V}(0) = 0$ and $\mathcal{V}(1) = 1$, Eq. (8) is solved numerically at various $\mathcal{J}$. The corresponding space-charge-limited current is determined when the value of $\mathcal{J}$ will cause the onset of $\mathcal{V}(\chi) < 0$, and the calculated SCLC $\mathcal{J}$ is plotted as a function of ϕ in Fig. 1(a), which exhibits contrasting behavior at $\phi \ll 1$ and at $\phi \gg 1$. For $\phi \ll 1$ [Fig. 1(b)] and $\phi \gg 1$ [Fig. 1(c)], the numerical results can be fitted by $\mathcal{J}'_{fit} = c_1 - c_2\phi$ and $\mathcal{J}''_{fit} = c_3/\sqrt{\phi}$, respectively, where $(c_1, c_2, c_3) = (0.889, 0.368, 1.092)$. The contrasting ϕ dependence can be understood from the dependence of $\phi \propto \rho_c$, which corresponds, respectively, to the ultrarelativistic SCLC at $\phi \ll 1$ (or small ϕ) and the nonrelativistic SCLC at $\phi \gg 1$ (or large ϕ). By substituting Eq. (9) into the above-mentioned fitting equations, $J_r \propto V^{3/2}/L^2$ and $J_{nr} \propto V^2/L^3$ are recovered, thus confirming the analytical solutions given in Eq. (5).

Figure 2 shows the smooth transition of V and L in between the ultrarelativistic and nonrelativistic regimes. The dimensionless current density $\tilde{J}_L$-$\tilde{V}$ characteristic (at a fixed L) exhibits a voltage scaling of $\alpha = 2$ at low $\tilde{V}$ and $\alpha = 3/2$ at

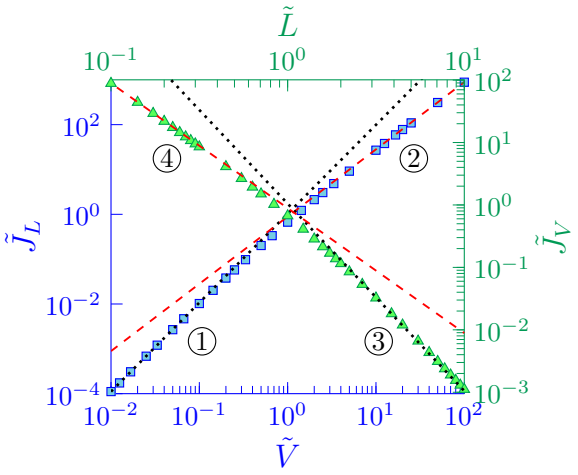

FIG. 2. Normalized voltage (blue axes, □ symbols) and length (green axes, △ symbols) characteristic of the current density. The broken (red) and dotted (black) guidelines represent the ultrarelativistic and nonrelativistic limit, respectively. The labels of the guidelines, i.e., 1, 2, 3, and 4, correspond to the scalings $\tilde{J}_L \propto V^2$, $\tilde{J}_L \propto V^{3/2}$, $\tilde{J}_V \propto L^2$, and $\tilde{J}_V \propto L^3$, respectively.

high $\tilde{V}$. Here the dimensionless parameters are $\tilde{J}_L \equiv \mathcal{J}/J_0$, $\tilde{V} \equiv V/V_0$, $J_0 \equiv \tau e^{3/2} v_F \sqrt{\epsilon\delta}/\hbar$, and $V_0 = \rho_c L^2/\epsilon\delta$. At a fixed L, we have $\tilde{V} \propto 1/V_0 \propto 1/\rho_c$, and thus low $\tilde{V}$ and high $\tilde{V}$ correspond to the nonrelativistic ($\tilde{J}_L \propto \tilde{V}^2$) and the ultrarelativistic ($\tilde{J}_L \propto \tilde{V}^{3/2}$) regimes, respectively, as shown in Fig. 2 (blue axis, □ symbols). In the intermediate regime, $\tilde{J}_L$-$\tilde{V}$ deviates from the simple power law, and applying a fitting would lead to a subquadratic scaling in the range of $3/2 < \alpha < 2$.

Similarly, the dimensionless $\tilde{J}_V$-$\tilde{L}$ characteristic (at a fixed V) shows a length scaling of $J \propto \tilde{L}^{-\beta}$ of $\beta = 2$ at small $\tilde{L}$ and $\beta = 3$ at large $\tilde{L}$, as shown in Fig. 2 (green axis, △ symbols). Here, the dimensionless parameters are $\tilde{J}_V = J/\bar{J}_0$, $\tilde{L} = L/L_0$, $\bar{J}_0 = \tau e^{3/2} v_F \rho_c V^{1/2}/\hbar\sqrt{\epsilon d}$, and $L_0 = \sqrt{\epsilon d V/\rho_c}$. As $\tilde{L} \propto \sqrt{\rho_c}$, small $\tilde{L}$ and large $\tilde{L}$ correspond to the nonrelativistic and the ultrarelativistic regimes, respectively. The $\beta < 3$ subcubic inverse length scaling represents another signature of the relativistic SCLC for Dirac solids in addition to the $\alpha < 2$ voltage scaling.

From Fig. 1(a), the numerical results over a wide range of ϕ can be accurately fitted by $\mathcal{J}_{\rm fit}(\phi) = \frac{a}{\sqrt{\phi}+b}$, where $(a,b) = (1.067, 1.450)$. As all parameters are intrinsically contained in $\mathcal{J}$ and ϕ, this empirical relation is universally valid and thus we derive a *master equation* that universally describes the SCLC transport over a wide range of parameters:

$$\frac{V^3}{I^2} = \frac{\Lambda(\rho_c,\epsilon d,\tau,L,W)}{V} + \Omega(\epsilon d,\tau,L,W), \qquad (10)$$

where $I = J \times W$ is the total current, W is the device width, and

$$\Lambda(\rho_c,\epsilon d,\tau,L,W) \equiv \frac{\rho_c}{(\epsilon d)^2}\frac{\hbar^2 L^6}{a^2\tau^2 v_F^2 e^3 W^2}, \qquad (11a)$$

$$\Omega(\epsilon d,\tau,L,W) \equiv \frac{b\hbar^2 L^4}{a^2\tau^2 v_F^2 e^3 W^2}\frac{1}{\epsilon d}. \qquad (11b)$$

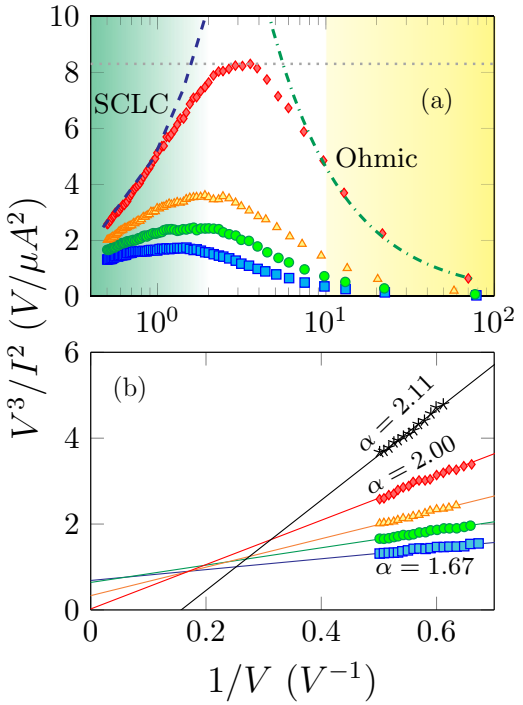

FIG. 3. Plot of V^3/I^2 against $1/V$ in the SCLC regime using MoS_2 experimental data from Ref. [31] with (T,α) of (285 K, 1.67) (blue square), (265 K, 1.73) (green circle), (245 K, 1.82) (yellow triangle), (205 K, 2.00) (red diamond), and (185 K, 2.11) (black star). (a) The entire V^3/I^2 range over $0.4 < 1/V < 100$. The green dash-dotted and blue dashed curves denote, respectively, Ohmic current ($J \propto V$) and SCLC ($J \propto V^2$) fitted to the $T = 205$ K data. The horizontal gray line indicates the transitional regime of $J \propto V^{3/2}$ ($1 < 1/V < 6$) separating the green-shaded SCLC-dominated and the yellow-shaded Ohmic-dominated regime. (b) The SCLC-dominated regime at small $1/V < 0.7$.

It is important to emphasize that Eq. (10) is extremely usefully if it is used to fit with the experimental I-V measurement (in the form of V^3/I^2 as a function of $1/V$) to determine the values of Λ and Ω, which can be subsequently used to determine the collision time scale τ by using Eqs. (9) if the other parameters are known.

For the ultrarelativistic limit at $\rho_c \to 0$, Eq. (10) becomes $V^3/I^2 \approx \Omega$, which confirms the *predicted* ultrarelativistic scaling of $(\alpha,\beta) = (3/2,2)$. For the nonrelativistic limit at $\rho_c \gg 0$, Eq. (10) reduces to $V^3/I^2 \approx \Lambda/V$, which recovers the classical MG scaling of $(\alpha,\beta) = (2,3)$ as expected. Therefore, the intermediate relativistic SCLC will produce a positive intercept on the vertical axis of V^3/J^2-$1/V$ characteristic, whereas the SCLC with nonrelativistic scaling will have a zero intercept, as shown in Fig. 3(b).

Interestingly, the V^3/I^2-$1/V$ characteristic [suggested in Eq. (10)] provides a convenient tool to represent the SCLC data that can be generally applied to any solids. To illustrate this point, we consider a trap-free solid in which the conduction transits from Ohmic to SCLC at increasing V, as shown in Fig. 3(a). In the Ohmic regime (large $1/V$ or small V) where $J \propto V$, we have $V^3/I^2 \propto (1/V)^{-1}$, i.e., V^3/I^2 decreases with increasing $1/V$ [green dash-dotted line in Fig. 3(a)]. In

contrast, in the SCLC regime (small $1/V$ or large V) where $I \propto V^2$, we have $V^3/I^2 \propto 1/V$, i.e., V^3/I^2 increases linearly with $1/V$ [blue dashed line in Fig. 3(a)]. These contrasting behaviors lead to a *transitional* peak [38] in the intermediate regime that clearly separates the SCLC-dominated and Ohmic-dominated conduction, as shown in Fig. 3(a). This finding is confirmed by using various experimental data (color symbols) for MoS_2 from Ref. [31] at different temperature, as shown in Fig. 3(a). The above-mentioned transitional peak between the SCLC-dominated regime (dashed curve) and the Ohmic-dominated regime (dash-dotted curve) can be clearly observed at all temperatures.

A zoom-in view at the small-$1/V$ SCLC-dominated regime is shown in Fig. 3(b), which indicates that the experimental results (symbols) can be explained by linear fitting to obtain the voltage scaling, which ranges from $\alpha = 2.11$ down to 1.67 according to Eq. (10). The α scaling decreases to $\alpha < 2$ at elevated temperature because the higher energy levels of the conduction band are increasingly populated by the thermally liberated electrons from trapping sites. This leads to a higher degree of relativistic dynamics of the transport electrons, thus reducing α. For the three $\alpha < 2$ cases, they can be extrapolated to have positive intercepts on the y axis at $1/V \to 0$ [see Fig. 3(b)]. As α approaches 2, the intercept diminishes and becomes approximately zero at $\alpha = 2$. These observations are in good agreement with the predicted intercepts of Eq. (10), as discussed above. Note that Eq. (10) breaks down in the case of $\alpha > 2$, where the intercept becomes negative.

III. SIMPLIFIED MODEL OF UNIFORM SCLC INJECTION IN A 2D DIRAC SEMICONDUCTOR

The relativistic SCLC model derived above is based on solving the 1D Poisson equation. The Dirac semiconductor is a 2D thin film, thus a 2D thin-form model is required. In this section, we provide a simplified formalism of the 2D thin-film relativistic SCLC model without the need to explicitly solve for the 2D model [8].

A. Universal model of D-dimensional uniform SCLC injection in a solid with density-dependent mobility

The SCLC has been previously formulated for thin films and nanowire using an integral form of the 2D electrostatic Poisson equation [8,10]. Here, we shall formulate a thin-film SCLC relativistic model under the assumption of carrier-density-dependent mobility to illustrate the general SCLC scaling properties for a Dirac semiconductor, which has a density-dependent mobility of $\mu_D = \gamma[en(x) + \rho_c]^{-1/2}$.

We consider the D-dimensional transport in a solid with density-dependent mobility in a general form of $\mu = \mu_0 f[n(x)]/f_0$, where $f[n(x)]$ is a density-dependent term and f_0 is a constant factor. The dimensionality of $D = 1$ and 2 corresponds to bulk and 2D thin film, respectively. In the following analysis, we consider the case of *uniform SCLC injection*, where the two electrodes are separated by a fixed spacing of L, as shown in Fig. 4(a). For uniform SCLC injection along the x direction, the electric field profiles, i.e.,

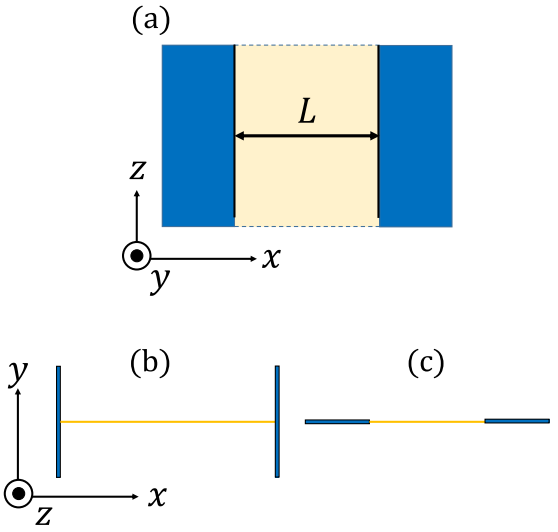

FIG. 4. Schematic drawings of the device and contact geometries. Top view of (a) is the constant-L contact geometry for uniform SCLC injection. Current is uniformly injected along the x direction. For $D = 1$ bulk geometry, the constant-L geometry is invariant along both the z and y directions, whereas for $D = 2$ thin-film geometry the structure is only invariant along the z direction. Parts (c) and (d) show the side view of constant-L 2D thin film with edge and strip contacts, respectively.

E_D for bulk ($D = 1$) and thin film ($D = 2$), can be written, respectively, as

$$E_1(x) = \frac{e}{\epsilon}\int dx' \frac{\partial G_1(x,x')}{\partial x} n_3(x'), \tag{12a}$$

$$E_2(x,y) = \frac{e}{\epsilon}\int dx' \int dy' \frac{\partial G_2(x,y,x',y')}{\partial x}\delta(y') n_2(x'), \tag{12b}$$

where $n_2(x)$ and $n_3(x)$ denote the surface and volume carrier density, respectively. $G_1(x,x')$ and $G_2(x,y,x',y')$ are, respectively, the 1D and 2D Green's functions that are dependent on the geometry of the contacts. Figures 4(b) and 4(c) show a 2D thin film with two possible contact geometries, i.e., edge and strip contacts, respectively [8]. By eliminating the y' integration via $\delta(y')$ and suppressing the argument of $y = 0$ in Eq. (12b) for simplicity, Eq. (12) can be written compactly as

$$E_D(\xi) = \frac{e}{\epsilon}\int_0^1 d\xi' \frac{\partial G_D(\xi,\xi')}{\partial \xi} n_\nu(\xi'), \tag{13}$$

where we have introduced a dimensionless variable as $\xi \equiv x/L$, and the subscript of $\nu = 2,3$ denotes surface and bulk carrier density, respectively. Considering that the charge-transport mechanism in a Dirac solid belongs to the class of density-dependent mobility models, we assume a general current density of

$$J_D = en_\nu(\xi)\mu_0 \frac{f[n_\nu(\xi)]}{f_0} E_D(\xi), \tag{14}$$

where the subscript $D = 1,2$ denotes linear and areal current density, respectively. The density-dependent mobility is given

as $\mu[n_\nu(\xi)] \equiv \mu_0 f[n_\nu(\xi)]/f_0$, where $f[n_\nu(\xi)]$ is an $n_\nu(\xi)$-dependent term and f_0 is a normalization constant. From Eq. (14), the bias voltage relation, $V = \int_0^L E_D(x')dx'$, is written as

$$J_D f_0 \int_0^1 \frac{d\xi'}{n_\nu(\xi') f[n_\nu(\xi')]} = e\mu_0 \frac{V}{L}. \tag{15}$$

The solution of Eq. (15) gives the equation of SCLC. Its full solution require knowledge of $n_\nu(\xi)$ over the intervals from $\xi = 0$ to 1, which can be obtained by solving the nonlinear integral equation in Eq. (13). Nonetheless, the scaling relations, i.e., J_D-V and J_D-L, can be readily deduced via a simple *dimensional analysis* [8] without explicitly solving Eqs. (13) and (15).

To illustrate this, we first combine Eqs. (13) and (14) to obtain

$$1 = \frac{e^2\mu_0}{\epsilon f_0 J_D} n_\nu(\xi) f[n_\nu(\xi)] \int_0^1 d\xi' \frac{\partial G_D(\xi,\xi')}{\partial \xi} n_\nu(\xi'). \tag{16}$$

From the Poisson equation, i.e., $\nabla^2 G_D(\mathbf{r},\mathbf{r}') = \delta_D(\mathbf{r})$, where $\delta_D(\mathbf{r})$ is a D-dimensional Dirac delta function, the physical dimension of G_D can be obtained as $[G_D(\xi,\xi')] = \mathcal{L}^{2-D}$, where $\mathcal{L}$ denotes the fundamental dimension of length, and $[X]$ denotes the unit of physical quantity X. Correspondingly, the partial derivative, $\partial G_D/\partial\xi$, in Eq. (16) can be nondimensionalized as

$$\frac{\partial G_D(\xi,\xi')}{\partial \xi} = L^{2-D} \frac{\partial \mathcal{G}_D(\xi,\xi')}{\partial \xi}, \tag{17}$$

where $\mathcal{G}_D(\xi,\xi')$ is a dimensionless Green's function. We now rewrite Eqs. (15) and (16) as

$$J_D f_0 \int_0^1 \frac{d\xi'}{n_\nu(\xi') f_\nu} = e\mu_0 \frac{V}{L}, \tag{18a}$$

$$1 = \left(\frac{e^2\mu_0 L^{2-D}}{\epsilon f_0 J_D}\right) n_\nu(\xi) f_\nu \int_0^1 d\xi' \frac{\partial \mathcal{G}_D(\xi,\xi')}{\partial \xi} n(\xi'), \tag{18b}$$

where $f_\nu \equiv f[n_\nu(\xi)]$ for simplicity. A direct inspection of Eq. (18a) shows that after the integral $\int d\xi'(\cdots)$ is fully converted into a dimensionless form, the J_D-V and J_D-L scaling relations can be unambiguously determined. In this case, $\int d\xi'(\cdots)$ becomes a *dimensionless numeric factor* that does not play any role in the J_D-V and J_D-L scaling relations.

The nondimensionalization of Eq. (18a) can be accomplished by appropriately regrouping the constant term in Eq. (18b), i.e., $(e^2\mu_0 L^{D-2}/\epsilon f_0 J_D)$, into each of the $n_\nu(x)$ and f_ν terms on the right-hand side of Eq. (18b) such that dimensionless terms $\mathcal{N}_\nu(\xi)$ and $\mathcal{F}_\nu$ can be defined, respectively, for $n_\nu(\xi)$ and f_ν. In general, the regrouping of $(e^2\mu_0 L^{D-2}/\epsilon f_0 J_D)$ can be expressed in an arbitrary form of

$$\frac{e^2\mu_0 L^{2-D}}{\epsilon f_0 J_D} \equiv \mathcal{A}_{J_D}(f_\nu)\tilde{\mathcal{A}}_{J_D}(f_\nu)\mathcal{B}_{L,D}(f_\nu)\tilde{\mathcal{B}}_{L,D}(f_\nu), \tag{19}$$

where $\mathcal{A}_{J_D}(f_\nu)$ and $\tilde{\mathcal{A}}_{J_D}(f_\nu)$ are terms containing J_D, and $\mathcal{B}_{L,D}(f_\nu)$ and $\tilde{\mathcal{B}}_{L,D}(f_\nu)$ are terms containing L^{2-D}. The roles of $\mathcal{A}$'s and $\mathcal{B}$'s are to pair up with $n(\xi)$ and f_ν in Eq. (18b) such that the resulting terms are dimensionless.

In the following, we suppress the argument of $\mathcal{A}$'s and $\mathcal{B}$'s for simplicity. As the explicit form of f_ν determines the regrouping of $(e^2\mu_0 L^{D-2}/\epsilon f_0 J_D)$, $\mathcal{A}$'s and $\mathcal{B}$'s are both f_ν-dependent. Furthermore, $\mathcal{A}$'s are D-independent and $\mathcal{B}$'s are D-dependent as L^{2-D} is deliberately distributed only into $\mathcal{B}$'s. We can now recast Eq. (18b) as

$$1 = \mathcal{N}_\nu(\xi)\mathcal{F}_\nu \int_0^1 d\xi' \frac{\partial \mathcal{G}_D}{\partial \xi} \mathcal{N}(\xi'), \tag{20}$$

where all terms are dimensionless via the following grouping:

$$\begin{aligned} \mathcal{N}_\nu(\xi) &\equiv (\mathcal{A}_{J_D}\mathcal{B}_{L,D}) n_\nu(\xi), \\ \mathcal{F}_\nu &\equiv (\tilde{\mathcal{A}}_{J_D}\tilde{\mathcal{B}}_{L,D}) f_\nu. \end{aligned} \tag{21}$$

With $\mathcal{N}_\nu(\xi)$ and $\mathcal{F}_\nu$ now being dimensionless, Eq. (18a) can be rewritten as

$$J_D \mathcal{A}_{J_D}\tilde{\mathcal{A}}_{J_D}\mathcal{B}_{L,D}\tilde{\mathcal{B}}_{L,D} \int_0^1 \frac{d\xi'}{\mathcal{N}_\nu(\xi')\mathcal{F}_\nu} = e\mu_0 \frac{V}{L}, \tag{22}$$

or more compactly as

$$J_D \mathcal{A}_{J_D}\tilde{\mathcal{A}}_{J_D} = \psi_{\mathcal{G}_D} \frac{e\mu_0}{\mathcal{B}_{L,D}\tilde{\mathcal{B}}_{L,D}} \frac{V}{L}, \tag{23}$$

where $\psi_{\mathcal{G}_D}$ is a dimensionless numeric factor dependent on D and $\mathcal{G}_D$, i.e.,

$$\psi_{\mathcal{G}_D} \equiv \left(\int_0^1 \frac{d\xi'}{\mathcal{N}_\nu(\xi')\mathcal{F}_\nu} \right)^{-1}, \tag{24}$$

which can be explicitly solved from Eq. (18b), and it affects only the overall magnitude of SCLC without affecting its voltage and length scaling relations. Thus the J_D-V and J_D-L scaling relations are determined by

$$J_D \mathcal{A}_{J_D}\tilde{\mathcal{A}}_{J_D} \propto \frac{1}{\mathcal{B}_{L,D}\tilde{\mathcal{B}}_{L,D}} \frac{V}{L}. \tag{25}$$

B. Derivation of 2D thin-film SCLC scaling relations

Equation (25) represents a *universal SCLC scaling relation* for uniform SCLC injection into either a $D = 1$ (bulk) or a $D = 2$ (thin film) based solid of length L with arbitrary density-dependent mobility $\mu[n_\nu(\xi)]$. Several remarkable properties can be extracted from Eq. (25): (i) The J_D-V scaling, i.e., $J_D \mathcal{A}_{J_D}\tilde{\mathcal{A}}_{J_D} \propto V$, is determined solely by the $\mu[n_\nu(\xi)]$ and is *completely independent of the device geometry* ($\mathcal{G}_D$) *and dimensionality* (D); (ii) the J_D-L scaling, on the other hand, is affected by both f_ν and D; (iii) for a fixed D (= 1 for bulk or = 2 for thin film), the geometry of contacts affects only $\psi_{\mathcal{G}_D}$ and hence both SCL J_D-V and J_D-L scaling are universally independent on contact.

From Eq. (19), we see that the constant term carries a length scale dependence of L^{2-D}, and thus Eq. (19) will be independent of L for $D = 2$ (for a thin-film setting) resulting in $\mathcal{B}_{L,2} = \tilde{\mathcal{B}}_{L,2} = 1$. In this 2D thin-film limit, Eq. (23) gives the SCLC relation for a thin film:

$$J_2 \mathcal{A}_{J_2}\tilde{\mathcal{A}}_{J_2} = \psi_{\mathcal{G}_2} e\mu_0 \left(\frac{V}{L}\right). \tag{26}$$

Note that Eq. (26) includes that both J_2-V and J_2-L follow the same scaling relation.

Together with property (i) and Eq. (26), a powerful tool is shown that can be used to directly map the scaling relation of a simple bulk SCLC model into the 2D thin-film SCLC model.

By virtue of property (i), we conclude that the voltage scaling for thin-film (J_2-V) is identical to the bulk J_1-V scaling, thus the voltage scaling obtained in Sec. II is valid for a thin film as well. For a thin film, Eq. (26) also dictates that the length (J_2-L) scaling relation is identical to the J_2-V scaling relation.

To summarize this section, we provide a rigorous derivation of scaling laws (both voltage and length) for uniform SCL injection into a 2D thin-film setting. These properties allow the J_2-V and J_2-L scaling relations of a 2D thin film to be fully determined from a simple 1D bulk SCLC model, which was shown in Sec. II. The full J_2-V and J_2-L scaling relations are thus obtained without the need of explicitly solving the complicated coupled equations in Eq. (18). In Appendix A, two examples of 2D thin-film SCLC are analyzed using our simplified formalism developed here.

C. Derivation of SCLC scaling relations and full numerical solutions of Eq. (18) for a 2D Dirac semiconductor with traps

The relativistic SCLC scaling relation of a Dirac semiconductor in 2D thin-film geometry can be readily determined by using the simple derivation developed above. Since the 1D SCLC scaling relation takes the form of $J_1 \propto V^{3/2}$ and $J_1 \propto V^2$, respectively, for the ultrarelativistic and nonrelativistic regimes, for 2D thin film our simple analysis yields

$$J_2 \propto \left(\frac{V}{L}\right)^{\alpha}, \tag{27}$$

where $\alpha = 2$ and 3/2 are for the nonrelativistic and ultrarelativistic limit, respectively. In the intermediate regime, the scaling follows an approximate power-law form with α varying continuously from 2 to 3/2 akin to Fig. 2.

To verify Eq. (27), the relativistic SCLC in 2D thin-film geometry with inclusion of exponential traps is explicitly solved (the full derivation is presented in Appendix B). In the presence of exponential traps, the relativistic SCLC in a 2D thin-film Dirac semiconductor is

$$\frac{n_s^l(\xi)(1-\xi^2)^{1/2}}{\sqrt{C_l n_s^l(\xi)+n_c}} = \int_{-1}^{1}\left(\frac{2\gamma e^2 C_l}{J_2\epsilon}\frac{n_s(\xi')(1-\xi'^2)^2}{\xi-\xi'} + \frac{\sqrt{C_l n_s^l(\xi)+n_c}}{\pi n_s^l(\xi')}\right)d\xi', \tag{28a}$$

$$V = \frac{J_2 L}{\gamma e C_l}\int_{-1}^{1}\frac{\sqrt{C_l n_s^l(\xi)+n_c}}{n_s^l(\xi)}d\xi, \tag{28b}$$

where $l \equiv T_c/T > 1$; $n_s(\xi)$ is the 2D carrier density; $n_c \equiv \rho_c/e$; $C_l \equiv N_0/N_t^l$, with N_0 as the effective density of states at the conduction-band edge and N_t as the trap density; and ξ and ξ' are dimensionless variables. In the ultrarelativistic and nonrelativistic SCLC regimes, we obtain $J_2 \propto (V/L)^{l/2+1}$ and $J_2 \propto (V/L)^{l+1}$, respectively. By setting $l = 1$ (which corresponds to a trap-free case), we obtain $J_2 \propto (V/L)^2$ (nonrelativistic) and $J_2 \propto (V/L)^{3/2}$ (ultrarelativistic), thus confirming the simple derivation in Eq. (27). This agreement demonstrates that the unconventional J_D-V scaling of $3/2 < \alpha < 2$ is a universal signature of the relativistic charge-carrier dynamics in both bulk and 2D thin-film geometries.

In comparison to prior works in Ref. [31], the variation of $\alpha \approx 1.7$ to $\alpha \approx 3$ with decreasing temperature was attributed to the transition from $T < T_c$ (valid) to $T > T_c$ (invalid). Our relativistic SCLC model with exponential traps presented here is intended, however, to take into account such a temperature dependence without imposing the invalid $T_c < T$ condition.

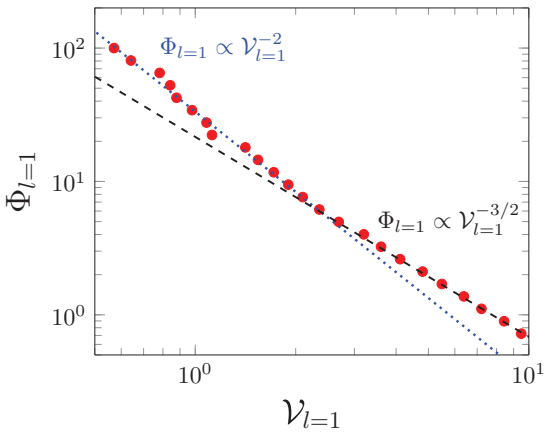

FIG. 5. Numerical solution of the trap-free ($l = 1$) 2D thin film of a Dirac semiconductor. The dashed and dotted lines denote $\Phi_{l=1} \propto \mathcal{V}_{l=1}^{-2}$ and $\Phi_{l=1} \propto \mathcal{V}_{l=1}^{-3/2}$, respectively. As $\Phi_{l=1} \propto 1/J_2$ and $\mathcal{V}_{l=1} \propto V/L$, the small-$\mathcal{V}_{l=1}$ and large-$\mathcal{V}_{l=1}$ regime corresponds to $J_2 \propto (V/L)^2$ (nonrelativistic) and $J_2 \propto (V/L)^{3/2}$ (ultrarelativistic), respectively. Note that the data points exhibit oscillations at small $\mathcal{V}_{l=1}$ due to a numerical error.

To further confirm the analytical relativistic SCLC scaling relation obtained above, the integral equation in Eq. (28a), which belongs to the class of *nonlinear Cauchy singular integral equations* [39], is numerically solved for the trap-free case of $l = 1$. The numerical solution $n_s(\xi)$ [from Eq. (28a)] is then integrated in Eq. (28b) to obtain J_2 as a function of V. For simplicity, Eq. (28) is solved in terms of a dimensionless variables, i.e., $\mathcal{V}_{l=1} \propto V/L$ and $\Phi_{l=1} \propto 1/J_2$ [see Appendix C and Eqs. (C6) and (C7) for the definition of $\mathcal{V}_l$ and Φ_l]. The numerical results (red circles) of $\Phi_{l=1}(\propto 1/J_2)$ as a function of $\mathcal{V}_l$ presented in Fig. 5 show good agreement with the derived scaling laws: $\Phi_{l=1} \propto \mathcal{V}_{l=1}^{-2}$ (dotted lines) at a small voltage of $\mathcal{V}_{l=1} < 2$, and $\Phi_{l=1} \propto \mathcal{V}_{l=1}^{-3/2}$ at a large voltage of $\mathcal{V}_{l=1} > 2$. Thus, the comparison confirms the two corresponding analytical scaling laws [see Eq. (27)] for space-charge-limited conduction in a 2D thin-film Dirac solid with a finite band gap: $J_2 \propto (V/L)^2$ and $J_2 \propto (V/L)^{3/2}$, respectively, for the nonrelativistic and ultrarelativistic limits. More importantly, the unconventional relativistic SCLC scaling of $3/2 < \alpha < 2$ is unambiguously confirmed for the 2D thin-film Dirac semiconductor and is in agreement with experiments [31,32].

Finally, we discuss the screening effect on the relativistic SCLC in 2D Dirac materials. In such materials, the charge transport is sensitively influenced by the substrate screening and excess charge screening induced by a gate electrode in field-effect-transistor geometry. Despite these screening effects, SCLC was unambiguously observed in experiments as reported in Refs. [31] and [32]. These experimental observations suggest that the screening effect cannot entirely remove SCLC in 2D materials. In a previous theoretical work [40], it was demonstrated that the surrounding dielectric screening will affect the transport properties of a 2D thin film

by modifying the relaxation time τ, and a significant mobility enhancement can be achieved via a high-dielectric substrate with a vanishingly thin membrane. This theoretical prediction was experimentally confirmed in monolayer MoS_2 with a high substrate [41]. With regard to our SCLC model, we point out that as the substrate screening effect alters only the relaxation time τ, which comes into the SCLC picture as a proportionality constant, it can be reasonably expected that only the magnitude of the SCLC will be altered while the new scaling laws reported here will remain unchanged. A microscopic theory of substrate screening can be formulated via first-principles calculation, which takes into account the complex many-body interactions at the interface between 2D materials and the substrate [42]. The complete microscopic quantum picture of dielectric screening is beyond the scope of this work.

IV. CONCLUSION

In summary, we have proposed a theory of relativistic space-charge-limited conduction (SCLC) in Dirac solids with new scaling laws for both bulk and thin file models. For the one-dimensional (1D) bulk model, the scaling laws are $J_1 \propto V^{\alpha}/L^{\beta}$ with $3/2 < \alpha < 2$ and $2 < \beta < 3$. For the 2D thin film model, we have $J_2 \propto (V/L)^{\alpha}$ for uniform SCLC injection with α remaining the same as the case of the 1D bulk model under the assumption of density-dependent mobility. Both scaling laws have been verified with numerical calculations and have good agreement with experimental results. The important finding from this paper is the new voltage scaling of $\alpha < 2$, which is a signature of the massive Dirac fermions in the 2D Dirac materials, and it cannot be explained by using the traditional SCLC models derived decades ago for traditional materials. The inconsistencies in using such traditional SCLC models with an unjustified trap condition to fit the experimental measurement is questionable. Our results represent another class of relativistic space-charge phenomena in Dirac solids that may be used to model Dirac-based devices operating in the space-charge-limited regime and may also be used as a tool to extract useful parameters by fitting the analytical equations with measurements. The relativistic SCLC model should generate unconventional SCL photocurrent response [11] in a relativistic Dirac semiconductor such as MoS_2. The widely studied photoresponse of MoS_2 [43] can be readily used as an additional platform to verify the proposed relativistic SCLC model here.

ACKNOWLEDGMENTS

We thank Subhamoy Ghatak for providing the experimental data of MoS_2 and for insightful discussions. We thank Chun Yun Kee, Kelvin J. A. Ooi, and Shi-Jun Liang for helpful discussions. This work is supported by Singapore Ministry of Education grant (T2MOE1401) and U.S. AFOAR (AOARD) Grant No. FA2386-14-1-4020.

APPENDIX A: TWO EXAMPLES OF 2D THIN-FILM SCLC USING THE SIMPLIFIED FORMALISM

In this appendix, we illustrate the simple derivation of the 2D SCLC scaling relations developed in Secs. III A and III B using two examples. In the first example, we consider a trivial case with $f_v/f_0 = 1$, i.e., the mobility is independent of carrier density. For the bulk model of $D = 1$, Eq. (18b) becomes

$$1 = \left(\frac{e^2\mu_0 L}{\epsilon J_1}\right)\int_0^1 d\xi' \frac{\partial \mathcal{G}_1(\xi,\xi')}{d\xi} n(\xi'), \tag{A1}$$

which can be fully nondimensionalized by defining $\mathcal{A}_J = (e^2\mu_0/\epsilon J_1)^{1/2}$, $\tilde{\mathcal{A}}_{J_1} = 1$, $\mathcal{B}_{L,1} = L^{1/2}$, and $\tilde{\mathcal{B}}_{L,1} = 1$. From Eq. (23), we obtained $J_1(e^2\mu_0/\epsilon J_1)^{1/2} = \psi_{\mathcal{G}_1} e\mu_0 V/L^{3/2}$, which can be rearranged to give the well-known bulk MG law of

$$J_1 = \psi_{\mathcal{G}_1}^2 \epsilon\mu_0 \frac{V^2}{L^3}. \tag{A2}$$

The numerical factor can be solved as $\psi_{\mathcal{G}_1}^2 = 9/8$ via Eq. (24) by using a 1D Green's function [8]. We can now map the J_1-V bulk SCLC scaling relation to the 2D thin-film case, which yields $J_2 \propto V^2$. Furthermore, as J_2-L scales equally with J_2-V, the 2D thin-film SCLC scaling relation can now be fully determined as $J_2 \propto (V/L)^2$. One can verify this scaling relation by explicitly solving Eq. (26) with $\mathcal{A}_{J_2} = (e^2\mu_0/J_2)^{1/2}$ and $\tilde{\mathcal{A}}_{J_2} = 1$. This gives $J_2(e^2\epsilon\mu_0/\epsilon J_2)^{1/2} = \psi_{\mathcal{G}_2} e\epsilon\mu_0 V/L$, which can be rearranged to give the well-known 2D thin-film SCLC [8], i.e.,

$$J_2 = \psi_{\mathcal{G}_2}\epsilon\mu_0\left(\frac{V}{L}\right)^2, \tag{A3}$$

where $\psi_{\mathcal{G}_2}$ is a $\mathcal{G}_2$-dependent numeric factor.

In the second example, we consider a carrier-density-dependent mobility in a power-law form, i.e., $f_v = n_v(\xi)^{l-1}$ and $f_0 = n_0^{l-1}$, where n_0 and l are some constants. This particular form of μ is equivalent to Mark-Helfrich's exponential-trap model with $l > 1$. For this particular form of f_v/f_0, Eq. (18b) can be fully nondimensionalized by regrouping the constant factor $(e^2\epsilon\mu_0 L/n_0^{l-1}J_1)$ via the following definitions: $\mathcal{A}_{J_1} = (e^2\epsilon\mu_0/n_0^{l-1}J_1)^{1/(l+1)}$, $\tilde{\mathcal{A}}_{J1} = (e^2\epsilon\mu_0/n_0^{l-1}J_1)^{(l-1)/(l+1)}$, $\mathcal{B}_{L,1} = L^{1/(l+1)}$, and $\tilde{\mathcal{B}}_{L,1} = L^{(l-1)/(l+1)}$. The bulk SCLC can then be obtained from Eq. (23) as

$$J_1\left(\frac{e^2\mu_0}{n_0^{l-1}\epsilon J_1}\right)^{\frac{l}{l+1}} = \psi_{\mathcal{G}_1} e\mu_0 \frac{V}{L^{\frac{2l+1}{l+1}}}, \tag{A4}$$

which can be simplified as

$$J_1 = \psi_{\mathcal{G}_1}^{l+1}\left(en_0^l\right)^{l-1}\epsilon^l\mu_0\frac{V^{l+1}}{L^{2l+1}} \tag{A5}$$

and is in agreement with the Mark-Helfrich exponential trap model [7]. To generalize the bulk SCLC to the case of 2D thin film, we again utilize the facts that (i) J_2-V follows the same scaling as J_1-V, and (ii) J_2-L scales equally with J_2-V. This gives $J_2 \propto (V/L)^{l+1}$, which is in agreement with the explicit solution of Eq. (26), i.e.,

$$J_2 = \psi_{\mathcal{G}_2}^{l+1}\left(en_0^l\right)^{l-1}\epsilon^l\mu_0\left(\frac{V}{L}\right)^{l+1}. \tag{A6}$$

APPENDIX B: DERIVATION OF THE 2D RELATIVISTIC SCLC MODEL

In this appendix, we provide a full derivation of the Mark-Helfrich SCLC model and Dirac semiconductor in 2D thin-film geometry based on Grinburg's formalism [8].

1. Mark-Helfrich's trap model of SCLC in 2D thin-film geometry

In the presence of traps that follow an exponential energy distribution [7], the free and trapped carrier densities are related by $n_f(x) = (N_0/N_t^l)n_s^l(x) \equiv C_l n_s^l(x)$, where $n_f(x)$ is the free carrier density, $n_s(x)$ is the trapped carrier density, N_0 is the effective density of states at the conduction-band edge, N_t is the trap density, and $C_l \equiv N_0/N_t^l$. Here, $l \equiv T_c/T \geqslant 1$, where T_c is a characteristic temperature representing the exponential spread in energy of the traps. The charge density in a 2D thin film is given as

$$\rho(x,y) = e\delta(y)[-n_s(x) + P_s\delta(L-x)], \tag{B1}$$

where $\delta(y)$ is a Dirac delta function and $P_s = \int_0^L n_s(x)dx$ is the charge density induced on the anode by the total $n_s(x)$ residing in the thin film. Note that y represents the direction that is out-of-plane of the thin film. For thin-edge contacts, the corresponding Green's function is

$$G(x-x',y-y') = -\frac{1}{2\pi}\ln[(x-x')^2+(y-y')^2]^{1/2} \tag{B2}$$

and the scalar potential can then be solved as

$$\phi(x,y) = -\frac{1}{2\pi}\int_{-\infty}^{\infty}dy'\int_0^L dx'\ln[(x-x')^2+(y-y')^2]^{1/2} \times\left(-\frac{4\pi e}{\epsilon}\right)\delta(y')[-n_s(x)+P_s\delta(L-x)]. \tag{B3}$$

Simplifying $\phi(x,y=0)$ and knowing that $E_x(x,0) = -d\phi/dx$, we obtain

$$E_x(x,0) = \frac{2e}{\epsilon(L-x)}\int_0^L \frac{L-x'}{x-x'}n_s(x')dx'. \tag{B4}$$

By defining $\xi = x/L$ and $\xi' = x'/L$, we obtained

$$E_x(\xi,0) = \frac{2e}{\epsilon(1-\xi)}\int_0^1 \frac{1-\xi'}{\xi-\xi'}n_s(\xi')d\xi'. \tag{B5}$$

We now consider a current density equation in Drude's form, i.e.,

$$J = en_f(x)\mu E_x(x,0). \tag{B6}$$

By combining Eqs. (B5) and (B6), we obtain

$$1 = \frac{2e^2\mu C_l}{J\epsilon}\frac{n_s(x)^l}{1-\xi}\int_0^1\frac{1-\xi'}{\xi-\xi'}n_s(\xi')d\xi'. \tag{B7}$$

Equation (B7) can be rearranged as follows:

$$1 = \left(\frac{2e^2\mu C_l}{J\epsilon}\right)^{\frac{l}{l+1}}\frac{n_s^l(\xi)}{1-\xi}\int_0^1\frac{1-\xi'}{\xi-\xi'}\left(\frac{2e^2\mu C_l}{J\epsilon}\right)^{\frac{1}{l+1}}n_s(\xi')d\xi'. \tag{B8}$$

By defining

$$\nu_s(\xi) \equiv \left(\frac{2e^2\mu C_l}{J\epsilon}\right)^{\frac{1}{l+1}}n_s(\xi), \tag{B9}$$

Eq. (B8) becomes

$$1 = \frac{\nu_s^l(\xi)}{1-\xi}\int_0^1\frac{1-\xi'}{\xi-\xi'}\nu_s(\xi')d\xi', \tag{B10}$$

which is an integral equation that can be solved to obtain $\nu(\xi)$. The bias voltage can be obtained from $V = \int_0^1 E_x(\xi,0)d\xi$ and Eq. (B6) as

$$V = \frac{JL}{e\mu C_l}\int_0^1\frac{d\xi}{n_s^l(\xi)}. \tag{B11}$$

To obtain the exponential trap-limited SCLC in 2D thin-film geometry with an edge contact, Eqs. (B9) and (B11) are combined to give

$$V = \frac{JL}{\epsilon\mu C_l}\left(\frac{2e^2\mu C_l}{J\epsilon}\right)^{\frac{1}{l+1}}\int_0^1\frac{d\xi}{\nu_s(\xi)}. \tag{B12}$$

With the definition of $\lambda \equiv \int_0^1 d\xi/\nu_s(\xi)$, which is a constant that can be solved from the integral equation in Eq. (B10), we obtain

$$J = \left(\frac{\epsilon}{2\lambda}\right)^l e^2\mu C_l\left(\frac{V}{L}\right)^{l+1}. \tag{B13}$$

Equation (B13) gives the exponential trap-limited SCLC of a 2D thin film with edge-contact geometry [see Fig. 4(b)]. For strip geometry [see Fig. 4(c)], the electric field is given as

$$E_x(\xi) = \frac{2}{(1-\xi^2)^{1/2}}\left(\frac{e}{\epsilon}\int_{-1}^1\frac{n_s(\xi')(1-\xi'^2)^{1/2}}{\xi-\xi'}d\xi' + \frac{V}{\pi L}\right), \tag{B14}$$

where $\xi \equiv (2x-L)/L$ and $\xi' \equiv (2x'-L)/L$. Using a similar procedure, we obtain

$$\frac{J}{e\mu} = \frac{2C_l n_s^l(\xi)}{(1-\xi^2)^{1/2}}\left(\frac{e}{\epsilon}\int_{-1}^1\frac{n_s(\xi')(1-\xi'^2)^{1/2}}{\xi-\xi'}d\xi' + \frac{1}{\pi L}\frac{JL}{e\mu C_l}\int_0^1\frac{d\xi}{n_s^l(\xi)}\right), \tag{B15}$$

which can be simplified to

$$1 = \frac{\nu_s^l(\xi)}{(1-\xi^2)^{1/2}}\left(\int_{-1}^1\frac{\nu_s(\xi')(1-\xi'^2)^{1/2}}{\xi-\xi'}d\xi' + \frac{1}{\pi}\int_{-1}^1\frac{d\xi}{\nu_s^l(\xi)}\right). \tag{B16}$$

From Eq. (B12), the SCLC current density equation is obtained as

$$J = \left(\frac{\epsilon}{2\lambda'}\right)^l e^2\mu C_l\left(\frac{V}{L}\right)^{l+1}, \tag{B17}$$

where the numeric factor $\lambda' \equiv \int_{-1}^1 d\xi\,\nu_s(\xi)$ can be obtained by solving $\nu_s(\xi)$ from Eq. (B16). In summary, the 2D thin-film uniform injection of SCLC in the presence of exponential traps

follows the following scaling relation:

$$J \propto \left(\frac{V}{L}\right)^{l+1} \tag{B18}$$

for both edge- and strip-contact geometries. More importantly, this scaling relation is in agreement with Eq. (A6) obtained using the simplified formalism.

2. Relativistic SCLC model for 2D massive Dirac fermions

For a 2D Dirac semiconductor, we obtain

$$1 = \frac{2\gamma e^2 C_l n_s^l(\xi)}{J\epsilon\sqrt{C_l n_s^l(\xi)+n_c}} \int_0^1 \frac{1-\xi'}{\xi-\xi'} n_s(\xi')d\xi' \tag{B19}$$

and

$$\frac{\sqrt{C_l n_s^l(\tilde{\xi})+n_c}(1-\tilde{\xi}^2)^{1/2}}{n_s^l(\tilde{\xi})} = \int_{-1}^1 \left(\frac{2\gamma e^2 V_l}{J\epsilon}\frac{n_s(\tilde{\xi}')(1-\tilde{\xi}'^2)^2}{\tilde{\xi}-\tilde{\xi}'} + \frac{\sqrt{C_l n_s^l(\tilde{\xi})+n_c}}{\pi n_s^l(\tilde{\xi}')}\right)d\tilde{\xi}', \tag{B20}$$

respectively, for edge-contact and strip-contact geometries. The applied bias voltage for edge- and strip-contact geometries becomes, respectively,

$$V = \frac{JL}{\gamma e C_l}\int_0^1 \frac{\sqrt{C_l n_s^l(\xi)+n_c}}{n_s^l(\xi)}d\xi \tag{B21}$$

and

$$V = \frac{JL}{\gamma e C_l}\int_{-1}^1 \frac{\sqrt{C_l n_s^l(\tilde{\xi})+n_c}}{n_s^l(\tilde{\xi})}d\tilde{\xi}. \tag{B22}$$

The coupled Eqs. (B19)–(B22) can be solved to obtain the relativistic SCLC in 2D thin-film geometry. Equations (B19)–(B22) have to be solved numerically. Nonetheless, in the nonrelativistic and ultrarelativistic limits, semianalytical scaling relations can be derived. We first consider the nonrelativistic limit of $n_c \gg n_s^l(\xi)$ for all ξ with edge contacts. Equations (B19) and (B21) can be approximated, respectively, by

$$1 = \frac{2\gamma e^2 C_l n_s^l(\xi)}{J\epsilon n_c^{1/2}}\int_0^1 \frac{1-\xi'}{\xi-\xi'} n_s(\xi')d\xi' \tag{B23}$$

and

$$V = \frac{JLn_c^{1/2}}{\gamma e C_l}\int_0^1 \frac{d\xi}{n_s^l(\xi)}. \tag{B24}$$

By defining

$$\nu_s(\xi) \equiv \left(\frac{2\gamma e^2 C_l}{J\epsilon n_c^{1/2}}\right)^{\frac{1}{l+1}} n_s(\xi), \tag{B25}$$

we obtain

$$J = \frac{1}{\lambda^{l+1}}\left(\frac{\epsilon}{2}\right)^l \frac{\gamma C_l}{n_c^{l/2}e^{2l-1}}\left(\frac{V}{L}\right)^{l+1}, \tag{B26}$$

where $\lambda \equiv \int_0^1 d\xi/\nu_s^l(\xi)$ is a numerical factor that can be solved from the nonlinear integral equation in Eq. (B19). By setting $l = 1$, the current-voltage scaling relation agrees with the 1D bulk model as shown in Eq. (5a) of the main text. The current voltage scales equally with the current length, which is also in agreement with the simplified derivation of the 2D thin-film SCLC scaling relation presented in Eq. (27) of the main text.

In the ultrarelativistic limit of $n_c \to 0$, Eqs. (B19) and (B21) become, respectively,

$$1 = \nu_s^{l/2}(\xi)\int_0^1 \frac{1-\xi'}{\xi-\xi'}\nu_s(\xi')d\xi' \tag{B27}$$

and

$$V = \frac{JL}{\gamma e}\left(\frac{2\gamma e^2 C_l^{1/2}}{J\epsilon}\right)^{\frac{l/2}{l/2+1}}\int_0^1 \frac{d\xi}{\nu_s^{l/2}(\xi)}, \tag{B28}$$

where

$$\nu_s(\xi) \equiv \left(\frac{2\gamma e^2 C_l^{1/2}}{J\epsilon}\right)^{\frac{1}{l/2+1}} n_s(\xi), \tag{B29}$$

which can be rearranged to give

$$J = \frac{1}{\lambda'^{l/2+1}}\left(\frac{\epsilon}{2}\right)^{l/2}\frac{\gamma e^{1-l/2}}{C_l^{l/4}}\left(\frac{V}{L}\right)^{\frac{l}{2}+1}. \tag{B30}$$

The numerical factor, $\lambda' \equiv \int_0^1 d\xi/\nu_s^{l/2}(\xi)$, can again be solved from Eq. (B19). For $l = 1$, the current-voltage scaling relation agrees with the ultrarelativistic results in Eq. (5b) of the main text. In the intermediate regime, the scaling relation can be approximated by

$$J \propto (V/L)^{\Lambda}, \tag{B31}$$

where $\Lambda = l/2+1$ and $\Lambda = l+1$.

APPENDIX C: EQUATIONS (B28)–(B32) IN DIMENSIONLESS FORM

Equations (B28)–(B32) can be transformed into dimensionless form for numerical solution in Fig. 5. For *edge contacts*, we obtain

$$1 = \frac{\Phi_l}{1-\xi}\frac{f_s^l(\xi)}{\sqrt{f_s^l(\xi)+1}}\int_0^1 \frac{1-\xi'}{\xi-\xi'}f_s(\xi')d\xi' \tag{C1}$$

and

$$\mathcal{V}_l = \frac{1}{\Phi_l}\int_0^1 \frac{\sqrt{f_s^l(\xi)+1}}{f_s^l(\xi)}d\xi. \tag{C2}$$

For *strip contacts*, the dimensionless form yields

$$1 = \frac{f_s^l(\xi)}{\sqrt{f_s^l(\xi)+1}}\frac{1}{(1-\xi^2)^{1/2}}\int_{-1}^1 \left(\Phi_l f_s(\xi')\frac{(1-\xi'^2)^{1/2}}{\xi-\xi'} + \frac{1}{\pi}\frac{\sqrt{f_s^l(\xi')+1}}{f_s^l(\xi')}\right)d\xi' \tag{C3}$$

and

$$\mathcal{V}_l = \frac{1}{\Phi_l}\int_{-1}^1 \frac{\sqrt{f_s^l(\xi)+1}}{f_s^l(\xi)}d\xi. \tag{C4}$$

The dimensionless parameters are defined as

$$f_s \equiv \frac{C_l}{n_c}^{1/l} n_s(\xi), \tag{C5}$$

$$\Phi_l \equiv \frac{2\gamma e^2}{J\epsilon}\left(\frac{n_c}{C_l}\right)^{1/l}\sqrt{n_c}, \tag{C6}$$

and

$$\mathcal{V}_l \equiv \frac{\epsilon V}{2eL}\left(\frac{C_l}{n_c}\right)^{1/l}, \tag{C7}$$

where Φ_l is a current- and material-dependent parameter.

[1] M. A. Lampert and P. Mark, *Charge Injection in Solids* (Academic, New York, 1970).

[2] N. F. Mott and R. W. Gurney, *Electronic Processes in Ionic Crystals* (Oxford University Press, New York, 1940).

[3] C. D. Child, Phys. Rev. (Series I) **32**, 492 (1911); I. Langmuir, Phys. Rev. **21**, 419 (1923).

[4] Y. B. Zhu, P. Zhang, A. Valfells, L. K. Ang, and Y. Y. Lau, Phys. Rev. Lett. **110**, 265007 (2013).

[5] L. K. Ang, T. J. T. Kwan, and Y. Y. Lau, Phys. Rev. Lett. **91**, 208303 (2003).

[6] Y. Y. Lau, D. Chernin, D. G. Colombant, and P.-T. Ho, Phys. Rev. Lett. **66**, 1446 (1991).

[7] P. Mark and W. Helfrich, J. Appl. Phys. **33**, 205 (1961).

[8] A. A. Grinberg, S. Luryi, M. R. Pinto, and N. L. Schryer, IEEE Trans. Electron Dev. **36**, 1162 (1989).

[9] W. Chandra, L. K. Ang, and K. L. Pey, Appl. Phys. Lett. **90**, 153505 (2007).

[10] A. A. Talin, F. Leonard, B. S. Swartzentruber, X. Wang, and S. D. Hersee, Phys. Rev. Lett. **101**, 076802 (2008).

[11] A. M. Goodman and A. Rose, J. Appl. Phys. **42**, 2823 (1972); V. D. Mihailetchi, J. Wildeman, and P. W. M. Blom, Phys. Rev. Lett. **94**, 126602 (2005).

[12] P. W. M. Blom, M. J. M. de Jong, and M. G. van Munster, Phys. Rev. B **55**, R656 (1997).

[13] L. Bozano, S. A. Carter, J. C. Scott, G. G. Malliaras, and P. J. Brock, Appl. Phys. Lett. **74**, 1132 (1999).

[14] A. J. Campbell *et al.*, Adv. Funct. Mater. **26**, 3720 (2016).

[15] T. N. Ng, W. R. Silveira, and J. A. Marohn, Phys. Rev. Lett. **98**, 066101 (2007).

[16] C. Tanase, E. J. Meijer, P. W. M. Blom, and D. M. de Leeuw, Phys. Rev. Lett. **91**, 216601 (2003).

[17] W. F. Pasveer, J. Cottaar, C. Tanase, R. Coehoorn, P. A. Bobbert, P. W. M. Blom, D. M. de Leeuw, and M. A. J. Michels, Phys. Rev. Lett. **94**, 206601 (2005).

[18] H. T. Nicolai, M. M. Mandoc, and P. W. M. Blom, Phys. Rev. B **83**, 195204 (2011).

[19] H. T. Nicolai, M. Kuik, B. de Boer, C. Campbell, C. Risko, J. L. Bredas, and P. W. M. Blom, Nat. Mater. **11**, 882 (2012).

[20] D. Abbaszadeh *et al.*, Nat. Mater. **15**, 628 (2016).

[21] X.-G. Zhang and S. T. Pantelides, Phys. Rev. Lett. **108**, 266602 (2012).

[22] J. Frenkel, Phys. Rev. **54**, 647 (1938); J. G. Simmons, *ibid.* **155**, 657 (1967).

[23] A. Rose, Phys. Rev. **97**, 1538 (1955).

[24] M. A. Lampert, Phys. Rev. **103**, 1648 (1956).

[25] A. Carbone, B. K. Kotowska, and D. Kotowski, Phys. Rev. Lett. **95**, 236601 (2005).

[26] A. K. Geim and K. S. Novoselov, Nat. Mater. **6**, 183 (2007).

[27] M. Z. Hasan and C. L. Kane, Rev. Mod. Phys. **82**, 3045 (2010); X. L. Qi and S.-C. Zhang, *ibid.* **83**, 1057 (2011).

[28] K. F. Mak, C. Lee, J. Hone, J. Shan, and T. F. Heinz, Phys. Rev. Lett. **105**, 136805 (2010).

[29] I. Jung, D. A. Dikin, R. D. Piner, and R. S. Ruoff, Nano Lett. **8**, 4283 (2008).

[30] D. Joung, A. Chunder, L. Zhai, and S. I. Khondaker, Appl. Phys. Lett. **97**, 093105 (2010).

[31] S. Ghatak and A. Ghosh, Appl. Phys. Lett. **103**, 122103 (2013).

[32] F. Mahvash, E. Parais, D. Drouin, T. Szkopek, and M. Siaj, Nano Lett. **15**, 2263 (2015).

[33] H. Bässler, Phys. Status Solidi B **175**, 15 (1993); S. V. Novikov, D. H. Dunlap, V. M. Kenkre, P. E. Parris, and A. V. Vannikov, Phys. Rev. Lett. **81**, 4472 (1998).

[34] G.-B. Liu, W.-Y. Shan, Y. Yao, W. Yao, and D. Xiao, Phys. Rev. B **88**, 085433 (2013); E. Cappelluti, R. Roldan, J. A. Silva-Guillen, P. Ordejon, and F. Guinea, *ibid.* **88**, 075409 (2013); Q. H. Wang, K. Kalantar-Zadeh, A. Kis, H. N. Coleman, and M. S. Strano, Nat. Nanotech. **7**, 699 (2012).

[35] G. W. Semenoff, Phys. Rev. Lett. **53**, 2449 (1984); R. M. Ribeiro and N. M. R. Peres, Phys. Rev. B **83**, 235312 (2011).

[36] In this limit, the density of states is $D(\varepsilon) = (m^*/2\pi\hbar^4)\Theta(\varepsilon - \Delta)$ and the carrier density is $n = (m^*/2\pi\hbar^4)(\mu - m^* v_F^2)$. Correspondingly, the current density is $J = (ne\tau/m^*)E$ and hence the SCLC reduces to the MG law, i.e., $J = (9\epsilon d\tau e/8m^*)V^2/L^3$. Note that this is different by a factor of 2 in comparison with Eq. (5). This is due to the different expansion scheme used in obtaining Eq. (5). The expansion of $[en(x) + \rho_c]^{-1/2}$ in Eq. (4) is performed *after* the **k** integration of the current density equation.

[37] L. K. Ang, Y. Y. Lau, and T. J. T. Kwan, IEEE Trans. Plasma Sci. **32**, 410 (2004).

[38] At the transitional regime where I is approximately proportional to $V^{3/2}$, V^3/I^2 becomes constant. This leads to the occurrence of a peak in the V^3/I^2-$1/V$ plot.

[39] E. G. Ladopoulos, *Singular Integral Equations* (Springer, New York, 2000).

[40] D. Jena and A. Konar, Phys. Rev. Lett. **98**, 136805 (2007).

[41] B. Radisavljevic, A. Radenovic, J. Brivio, V. Giacometti, and A. Kis, Nat. Nanotech. **6**, 147 (2011).

[42] N. Kharche and V. Meunier, J. Phys. Chem. Lett. **7**, 1526 (2016).

[43] O. Lopez-Sanchez, D. Lembke, M. Kayci, A. Radenovic, and A. Kis, Nat. Nanotech. **8**, 497 (2013); M. Buscema *et al.*, Nano Lett. **14**, 3347 (2014).